Astronomy
&
Astrophysics

Ultraviolet-to-far infrared properties of Lyman break galaxies and luminous infrared galaxies at *z* ~ 1

D. Burgarella[1], P. G. Pérez-González[2], K. D. Tyler[2], G. H. Rieke[2], V. Buat[1], T. T. Takeuchi[1,*], S. Lauger[1],
S. Arnouts[1], O. Ilbert[3], T. A. Barlow[4], L. Bianchi[5], Y.-W. Lee[6], B. F. Madore[7,8],
R. F. Malina[1], A. S. Szalay[9], and S. K. Yi[6]

[1] Observatoire Astronomique Marseille Provence, Laboratoire d'Astrophysique de Marseille, traverse du siphon,
13376 Marseille Cedex 12, France
e-mail: [denis.burgarella;veronique.buat;tsutomu.takeuchi;sebastien.lauger]@oamp.fr
[2] Steward Observatory, University of Arizona, 933 North Cherry Avenue, Tucson, AZ 85721, USA
e-mail: [pgperez;ktyler;grieke]@as.arizona.edu
[3] Osservatorio Astronomico di Bologna, via Ranzani, 1 - 47 Bologna, Italy
e-mail: olivier.ilbert1@bo.astro.it
[4] California Institute of Technology, MC 405-47, 1200 E. California Boulevard, Pasadena, CA 91125, USA
e-mail: tab@srl.caltech.edu
[5] Center for Astrophysical Sciences, The Johns Hopkins University, 3400 North Charles St., Baltimore, MD 21218, USA
e-mail: bianchi@skyrv.pha.jhu.edu
[6] Center for Space Astrophysics, Yonsei University, Seoul 120-749, Korea
e-mail: [ywlee;yi]@galaxy.yonsei.ac.kr
[7] Observatories of the Carnegie Institution of Washington, 813 Santa Barbara Street, Pasadena 91101, USA
e-mail: barry@ipac.caltech.edu
[8] NASA/IPAC Extragalactic Database, California Institute of Technology, Mail Code 100-22, 770 S. Wilson Ave.,
Pasadena, CA 91125, USA
[9] Department of Physics and Astronomy, Johns Hopkins University, 3400 North Charles Street, Baltimore, MD 21218, USA
e-mail: szalay@tardis.pha.jhu.edu

ABSTRACT

Aims. We present the first large, unbiased sample of Lyman Break Galaxies (LBGs) at $z \sim 1$. Far ultraviolet-dropout (1530 Å) galaxies in the Chandra Deep Field South have been selected using *GALEX* data. This first large sample in the $z \sim 1$ universe provides us with a high quality reference sample of LBGs.
Methods. We analyzed the sample from the UV to the IR using *GALEX*, *SPITZER*, *ESO* and *HST* data.
Results. The morphology (obtained from GOODS data) of 75% of our LBGs is consistent with a disk. The vast majority of LBGs with an IR detection are also Luminous Infrared Galaxies (LIRGs). As a class, the galaxies not detected at 24 μm are an order of magnitude fainter relative to the UV compared with those detected individually, suggesting that there may be two types of behavior within the sample. For the IR-bright galaxies, there is an apparent upper limit for the UV dust attenuation and this upper limit is anti-correlated with the observed UV luminosity. Previous estimates of dust attenuations based on the ultraviolet slope are compared to new ones based on the FIR/UV ratio (for LBGs detected at 24 μm), which is usually a more reliable estimator. Depending on the calibration we use to estimate the total IR luminosity, β-based attenuations $A_{\rm FUV}$ are larger by 0.2 to 0.6 mag. than the ones estimated from FIR/UV ratio. Finally, for IR-bright LBGs, median estimated β-based SFRs are $2-3$ times larger than the total SFRs estimated as $SFR_{\rm TOT} = SFR_{\rm UV} + SFR_{\rm IR}$ while IR-based SFRs provide values below $SFR_{\rm TOT}$ by 15–20%. We use a stacking method to statistically constrain the 24 μm flux of LBGs non individually detected. The results suggest that these LBGs do not contain large amounts of dust.

Key words. cosmology: observations – galaxies: starburst – ultraviolet: galaxies – infrared: galaxies – galaxies: evolution – galaxies: fundamental parameters

---

* *Present address*: Astronomical Institute, Tohoku University Aoba, Aramaki, Aoba-ku, Sendai 980-8578, Japan

1. Introduction

Lyman Break Galaxies (LBGs) are the most numerous objects observed at high redshift ($z > 2$–3) in the rest-frame ultraviolet (UV). The discovery of a large population of LBGs beginning with the work of Madau et al. (1996), followed by the spectral confirmation of their redshifts, provided the astronomical community with the first large sample of confirmed high redshift galaxies (Steidel et al. 1996; Lowenthal et al. 1997). The spectra of bright LBGs (e.g. cB58 by Pettini et al. 2000; Teplitz et al. 2000) are remarkably similar to those of local starbursts, indicating that these objects are forming stars at a high rate. The observed colors of LBGs are redder than expected for dust-free star-forming objects. This reddening suggests that some dust is present in this population. However, the amount of dust in LBGs (Baker et al. 2001; Chapman et al. 2000), and therefore the reddening-corrrected star formation rate (SFR^c), is poorly known. Meurer et al. (1999), Adelberger & Steidel (2000) and subsequent papers tried to estimate the amount of dust attenuation from the β method (Calzetti et al. 1994). However, it has been shown recently that this approach only provides rough estimates of the total UV attenuation in local galaxies (e.g. Buat et al. 2005; Burgarella et al. 2005; Seibert et al. 2005; Goldader et al. 2002 and Bell 2002).

High redshift LBGs are mainly undetected at submillimeter (sub-mm) wavelengths, where the emission of galaxies is dominated by the dust heated by young stars (Kennicutt 1998). Only the most extinguished LBGs are detected by SCUBA (Chapman et al. 2000; Ivison et al. 2005) and we have no idea of the dust attenuation for a representative sample. Very recently, Huang et al. (2005) observed a population of LBGs at $2 < z < 3$ detected with *SPITZER*. Unfortunately, due to the very high redshift, the *SPITZER/MIPS* observations were not deep enough to detect the thermally reradiated emission from very many LBGs at $z \sim 3$ and the *SPITZER/IRAC* data, although deep enough to detect many LBGs, only probe the rest-frame NIR (i.e. no information about the dust enshrouded star formation can be inferred). The morphology of LBGs is also a matter of debate: early works (e.g. Giavalisco et al. 1996) suggested that LBGs could be ellipsoidal, and therefore perhaps the progenitors of ellipticals or of the bulges of spiral galaxies. The problem is that we can hardly detect low surface brightness areas at high redshift because of the cosmological dimming. For instance, Burgarella et al. (2001) suggest that only compact star forming regions could be easily detected in deep *HST* observations.

On the other hand, observations in the sub-mm range have revealed a population of FIR-bright galaxies that might be similar to local (Ultra) Luminous IR galaxies ((U)LIRGs) (Blain et al. 1999) with $10^{11} L_\odot < L_{IR} = L(8 - 1000\,\mu m) < 10^{12} L_\odot$ for LIRGs and $10^{12} L_\odot < L_{IR} < 10^{13} L_\odot$ for ULIRGs. These objects are likely to dominate the Cosmic Infrared Background (CIB; Elbaz & Cesarsky 2003) at high redshift. The link between LBGs and LIRGs is still an open question: are there two classes of objects or are they related? If they are two facets of the same population, then we could, for instance, correct UV fluxes for the dust attenuation to recover the full Star Formation Density (e.g. Pérez-González et al. 2005).

The usual way of detecting and identifying LBGs is through the so-called dropout technique, i.e. the absence of emission in the bluest of a series of bands due to the Lyman break feature moving redwards with the redshift (e.g. Steidel & Hamilton 1993; Giavalisco 2002). However, it is well known that selection effects can have a very strong influence on the deduced characterics of an observed galaxy sample (e.g. Buat et al. 2005; Burgarella et al. 2005). Until now, there has been no way to detect a general, unbiased sample of LBGs at low redshift (i.e. $z \leq 2$), with the same dropout method very successfully used at $z \geq 2$ because we lacked an efficient observing facility in the UV range. This was quite unfortunate because the simple fact that the galaxies are closer to us means that we can access much more information on the morphology, detect fainter LBGs in the UV and in the IR, and therefore harvest larger samples. *GALEX* and *SPITZER* changed this situation and have allowed us to define a large sample of LBGs at $z \sim 1$ in the Chandra Deep Field South (CDFS).

In this study, we combine the detection in the UV of true (i.e. with a detected Lyman break) LBGs at $z \sim 1$ with *GALEX* and at 24 μm with SPITZER/MIPS. These data let us estimate the total dust emission and therefore, the dust-to-UV flux ratio, which provides a good tracer of the dust attenuation in the UV. We also use high spatial resolution images to analyse their morphology. We are therefore able to perform a complete analysis for the first time on a large LBG sample.

A cosmology with $H_0 = 70$ km s^{-1} Mpc^{-1}, $\Omega_M = 0.3$ and $\Omega_\Lambda = 0.7$ is assumed in this paper.

2. The galaxy sample

GALEX (Martin et al. 2005) observed the CDFS field for 44 668 s (Deep Imaging Survey = DIS) in both the far ultraviolet (FUV) and the near ultraviolet (NUV). The *GALEX* field is centered at α = 03h32m30.7s, δ = -27deg52$'$16.9$''$ (J2000.0). The *GALEX* IR1.1 pipeline identified 34610 objects within the 1.25°-diameter field of view. The GALEX resolution (image full width at half Maximum = *FWHM*) is about 4.5 arcsec in FUV and 6 arcsec in NUV.

This field has also been observed by *SPITZER* using MIPS (Rieke et al. 2004) in the guaranteed time observing program. The MIPS observations provide about 7$-$8 sources arcmin^{-2} at 24 μm centered on a $\sim 1.45 \times 0.4 = 0.6$ deg^2 field of view. The SPITZER image *FWHM* is about 6 arcsec and almost perfectly matches that of GALEX.

Redshifts from GOODS (Vanzella et al. 2005) and VVDS (Le Fèvre et al. 2004) are available at the center of the GALEX field. Part of the *GALEX* CDFS field was observed by COMBO 17 (Wolf et al. 2004) over 0.5×0.5 deg^2. We made use of COMBO 17 redshifts for objects with $r < 24.5$. In this range, the quality $\delta z/(1 + z)$ remains within $\sigma_z < 0.03$ for 53% of the objects. Finally, we obtained photometry from the European Southern Observatory Imaging Survey (EIS) in U, B, V, R and I.

We built a sample of LBGs as follows. From the sources with redshifts, we selected objects in the rest-frame FUV (i.e. in the observed NUV) that we cross-correlated ($r = 1$ arcsec) first with the ground-based optical EIS data, then ($r = 4$ arcsec)
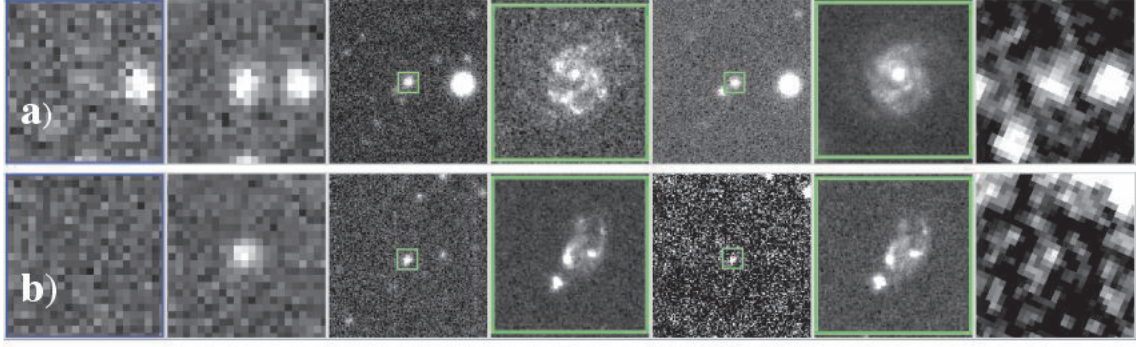
Fig. 1. Two galaxies from our LBG sample are shown here, from left to right in *GALEX* FUV and NUV, then *EIS* B, *HST* GOODS B, *EIS* I, *HST* GOODS I and finally *SPITZER/MIPS* 24 μm band. For the two galaxies, the leftmost image (blue frame) is below the Lyman break at $z \sim 1$ and the galaxy is not visible. The size of GOODS images is 4×4 arcsec^2. The corresponding GOODS field (green frame) is plotted in the large (35×35 arcsec^2) *EIS* images. **a)** a LBG classified as a disk-dominated galaxy; the more compact object is at $z = 0.546$ from VVDS, it appears reddish and should not contribute in ultraviolet and in far infrared; **b)** a LBG classified as a merger / interacting galaxy.

with the MIPS 24 μm data. In the resulting catalogue, we down-selected to objects that COMBO 17 puts in the "GALAXY" class. Then, we extracted the sources with redshift $0.9 \leq z \leq 1.3$. Since we wish to study Lyman break galaxies, we omitted objects without observed NUV and U flux: we kept only objects down to GALEX NUV magnitudes = 24.5 corresponding to the GALEX 80% completeness level and the U-band limiting magnitude at $U = 25.1$. We did not use a color–color selection as performed by Steidel & Hamilton (1993). Since we are studying galaxies with known redshifts, the extra color is not needed to screen out interlopers. The selection on the x-axis (i.e. $G - R$ color) might bias the sample toward low-reddening LBGs that we wish to avoid so we can achieve a more general understanding of the sample. In fact, we find that the members of our sample fall within the traditional color–color LBG range, or very close to it, as discussed in Sect. 3.5. For galaxies at $z \sim 1$, *GALEX* FUV corresponds to a rest-frame wavelength of ∼765 Å and *GALEX* NUV corresponds to ∼1155 Å. The observed FUV and NUV filters are therefore in the same rest-frame wavelength ranges as U and G filters used to identify Lyman breaks at high redshift (e.g. Giavalisco 2002 for a review). The observed FUV-NUV color thus gives a clear indication of the Lyman break. We picked the objects with the strongest indication of a break: FUV − NUV > 2; the final sample contains 297 LBGs. Of this list, 49 objects (16.5%) have a measured flux above the 80% completeness limit of the *SPITZER* 24 μm data (e.g. Pérez-González et al. 2005) and thus at a high enough ratio of signal to noise to be treated individually. Figure 1 shows two examples of these LBGs at several wavelengths including the two *GALEX* bands, the B and R EIS bands and the 24 μm *SPITZER/MIPS* band. Many additional galaxies were detected by *SPITZER* but at a weaker level; below we will describe how we used a stacking technique to probe their properties. Our sample of 297 UV-selected LBGs in the redshift range $0.9 \leq z \leq 1.3$ constitutes the database that we will study in this work (except for Sect. 3.5). The common *GALEX – SPITZER/MIPS –* COMBO 17 field of view (mainly limited by COMBO 17) is about 0.25 deg^2, which translates to ∼1180 LBGs deg^{-2} and ∼200 LBGs deg^{-2} for which we have individual IR detections.

3. Lyman break galaxies at z ∼ 1

Our LBGs provide the first opportunity to study an unbiased sample of LBGs systematically at $z \sim 1$. We analyze the UV and IR luminosities of these galaxies, measure their morphologies and their star formation as revealed by the UV and IR data and finally discuss the implications they have for studies centered on higher redshifts.

3.1. Ultraviolet and infrared luminosities

We find a large range of observed (i.e. un-corrected for dust attenuation) FUV luminosities (λf_λ in rest-frame FUV) with $9.3 \leq \mathrm{Log}\, L_{\mathrm{UV}}[L_\odot] \leq 11.0$. The lowest luminosity is set by the limiting magnitude in the U-band at $U = 25.1$. Below the break, the limiting magnitude amounts to FUV = 26.0. Although fainter objects are detected in the NUV (down to NUV = 25.9), we use a limiting magnitude of NUV = 24.5 to compute safer FUV − NUV colors and therefore perform a safer Lyman Break selection. The average value is $\langle \mathrm{Log}\, L_{\mathrm{UV}}[L_\odot] \rangle = 10.2 \pm 0.3$ for the sample with individual IR detections, and $\langle \mathrm{Log}\, L_{\mathrm{UV}}[L_\odot] \rangle = 10.1 \pm 0.3$ for the rest of the sample.

Total IR luminosities (L_{IR}) are estimated following the procedure described in Pérez-González et al. (2005). Briefly, rest-frame 12 μm fluxes are calculated by comparing the observed mid-IR SEDs (including IRAC and MIPS fluxes) of each individual galaxy with models of dust emission (e.g. Chary & Elbaz 2001; or Dale et al. 2002). This procedure is meant to cope with the strong K-corrections observed in the mid-IR due to the emission from aromatic molecules. We use the formulations of Takeuchi et al. (2005) and Chary & Elbaz (2001) for conversion from 12 μm flux density to L_{IR}. In addition to the intrinsic differences due to the two calibrations (the former provides L_{IR} lower by 0.2 dex), the conversion from $L_{12\,\mu m}$ to L_{IR} can introduce errors up to a factor of 2 for individual normal galaxies and 4 for galaxies with SED variations over the full IRAS sample range (Takeuchi et al. 2005; Dale et al. 2005). The effects of these errors are greatly reduced in this work because we discuss average properties, not those of individual
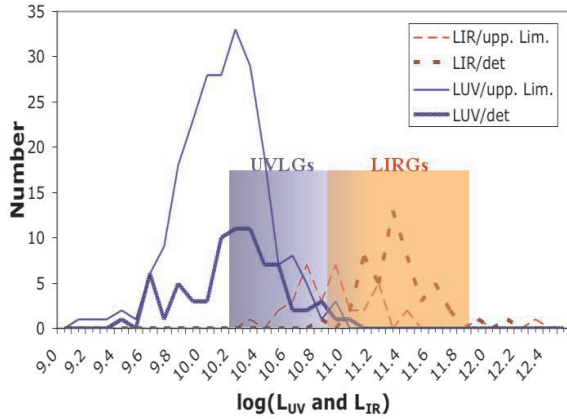
Fig. 2. The distribution in observed luminosity presented here corresponds to UV luminosities in blue (solid) and IR luminosities in red (dashed). Heavy lines are drawn from the population of LBGs with detected counterparts in the 24 μm MIPS image and thin lines to upper limits only. Note that the cut at low L_{IR} is not sharp because the 83 μJy limit used here is not the detection limit but the 80% completeness limit. UV luminosities cover the same range for the two samples and reach uncorrected UV luminosities of Log L_{UV} = 11 (in $L_\odot$). This upper limit is consistent with Adelberger & Steidel range for LBGs at $z \sim 3$ but seems inconsistent with the Balmer-break sample at $z \sim 1$. Two areas are shaded. Starting from the left, the first corresponds to the range covered by UV Luminous Galaxies (open right ended) and the second one corresponds to Luminous IR Galaxies. A few Ultra Luminous IR Galaxies are also detected.

Fig. 3. The morphology of the LBG sample is quantitatively estimated from the asymmetry and the concentration (sub-sample drawn from a larger CDFS analysis by Lauger et al. 2005b). The smaller number of objects presented here is due to the smaller field of view of *GOODS* as compared to ours. Black circless are LBGs without IR counterparts while red diamonds represent LBGs with a 24 μm MIPS detection. The line corresponding to the limit between disk-dominated and bulge-dominated galaxies (Lauger et al. 2005a). The location in the diagram reflects the morphological type of the galaxies: more asymmetrical LBGs (e.g. mergers) are in the top part of the diagram ($A > 0.25$) while early-type spirals would have $A < 0.1$. The LBG sample is mainly dominated (75%) by disk-dominated galaxies and the contribution from mergers amounts to ∼21%.

galaxies; in this case, the uncertainties are likely to be commensurate with those in the overall conversions to L_{IR} (i.e., still ∼0.2 dex). There are also uncertainties in the luminosity values due to the distance (since we use photometric redshifts with $\delta z/(z + 1) \leq 0.03$), but they are less than 10% for L_{UV} and L_{IR}.

It is difficult to compare our sample to previously published ones since none was available in this redshift range before *GALEX*. However, Adelberger & Steidel (2000) have discussed a Balmer-break sample at $z \sim 1$. The distributions in L_{UV} and L_{IR} for our sample are shown in Fig. 2. The lower limit is set by the flux limits but the upper limit of our LBG sample is about the same as the $z > 3$ one in Adelberger & Steidel's (2000). However, the upper limit of our sample is higher by a factor of ∼4 (assuming $H_0 = 70$) than Adelberger & Steidel's (2000) sample.

Heckman et al. (2005) defined UV Luminous Galaxies (UVLGs) as galaxies with UV luminosities above Log (L_{UV}) = 10.3 $L_\odot$. They found that these UVLGs bear similarities to LBGs, especially a sub-sample of compact ones. In our sample, 22.2% of the LBGs are UVLGs, 30.6% of the LBGs with an IR counterpart are UVLGs. The 83 μJy detection limit at 24 μm approximately corresponds to Log $(L_{IR}) \geq 11$ $L_\odot$, that is, nearly all the IR-detected LBGs are LIRGs (95.9%) and there are 2 ULIRGs (4.1%). An association between UVLGs and LIRGs was proposed by Burgarella et al. (2005). We confirm here this association and extend it to LBGs.
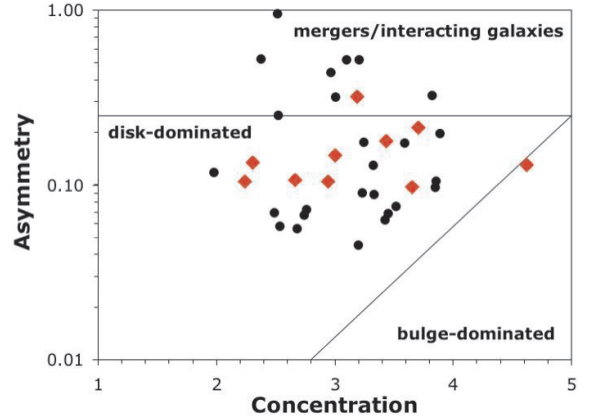
3.2. The morphology

The Great Observatories Origins Deep Survey (GOODS) provides high resolution and high signal-to-noise images of some of our LBGs, which can be used to study their morphology in the rest-frame *B* band. An advantage of our low redshift sample of LBGs is that the images extend to low surface brightness and hence morphologies can be determined well. We compute the asymmetry and concentration (Fig. 3) as in Lauger et al. (2005a) from the objects within the GOODS field which have a signal-to-noise ratio larger than $S/N \approx 1$ per pixel and whose coordinates are within 2 arcsec from the GALEX detection. We were able to obtain the morphology for only 36 LBGS out of our 297 LBGs (about 1/4 of our GALEX + SPITZER + COMBO 17 field is covered by GOODS). Figure 3 leads us to two conclusions: i) all but one LBG in our sample are located on the disk side of the line separating disk-dominated and bulge-dominated galaxies, and ii) part of them (22%) are in the top part of the diagram, i.e. with an Asymmetry larger than 0.25 and could be interpreted as mergers. This kind of quantitative analysis is also applied to higher redshift LBGs, however, we must be careful in the interpretation because, even if disks are present, it would be very difficult to detect them due to the cosmological dimming (e.g. Burgarella et al. 2001). Indeed, in deep spectroscopic observations (e.g. Moorwood et al. 2000; Pettini et al. 2001), the profiles of the optical nebular lines suggest the presence of disks in some LBGs.

A number of studies have been devoted to galaxy morphology in the redshift range $0.6 \leq z \leq 1.2$. At $z \sim 0.7$, most of the works seem to agree that about 60−70% of the objects can be classified as disk-dominated galaxies (mainly spirals

and Magellanic irregulars) and 10−20% as mergers/interacting galaxies. Here spirals are a sub-group of disks which exhibit a more symmetric (spiral) structure than irregular-like objects similar to the Magellanic clouds. Their asymmetry is therefore lower. Lauger et al. (2005b) found about 70−80% of disk-dominated galaxies at $z \sim 1$. Zheng et al. (2004) studied the *HST* morphology of a sample of LIRGs and also found that a large majority (~85%) of them are associated with disk-dominated galaxies. This conclusion is reached whether the selection is in the rest-frame ultraviolet (Wolf et al. 2005) or in the infrared (Bell et al. 2005). However, some dispersion due to the cosmic variance might exist (Conselice et al. 2005).

Therefore, overall it appears that the majority of the star formation at $0.6 < z < 1$ resides in disks and about half of it in spirals. The numbers that we draw for our LBG sample at $z \sim 1$ are globally consistent: we find that ~22% of the LBGs are likely mergers (e.g. Fig. 1b), ~75% are disks (e.g. Fig. 1a) and only ~3% (i.e. 1 galaxy) is possibly a spheroid. In the cases where our LBGs can also be classified as LIRGS from their IR luminosity, our measured morphologies are consistent with the LIRG morphology measurements of Zheng et al. (2004).

3.3. Ultraviolet dust attenuations

Until now, it has been difficult to estimate the validity of dust attenuation estimates for distant LBGs, because we had no clear idea of their L_{IR}. Adelberger & Steidel (2000) tried to estimate the 800 μm fluxes of their LBG sample from the β method and compared the results to observations. However, only the most extreme LBGs can be detected either directly in the sub-millimeter range or in the radio range at 1.4 GHz and therefore could be used in this comparison.

In this paper, we use total IR luminosities, L_{IR}, and L_{UV} to compute the FIR/UV ratio, which is calibrated into FUV dust attenuation A_{FUV} (e.g. Burgarella et al. 2005). This method has been shown to provide more accurate dust attenuations than those from the UV slope β. Figure 4 shows an apparent anti-correlation of A_{FUV} with the UV luminosity. It is not clear, however, whether this relationship is real or only observational. Indeed, in addition to the observational cut at low L_{FUV}, the 24 μm lower limiting flux means that we cannot detect individually low-luminosity galaxies with low dust attenuations. It is very interesting to note that we do not detect LBGs with both a high UV luminosity and a high UV dust attenuation, and this cannot be caused by observational limits. In other words, we seem to observe a population of high L_{UV} LBGs (which qualify as UVLGs) with dust attenuations similar to UV-selected galaxies in the local universe (e.g. Buat et al. 2005). UVLG galaxies are LIRGs with the lowest A_{FUV}.

There are now studies of high-redshift LBGs ($z > 2$) with *SPITZER* (e.g. Labbé et al. 2005; Huang et al. 2005). However, the results are so far inconsistent: Labbé et al. (2005) found that LBGs are consistent with low-reddening models while Huang et al. (2005) found more reddened LBGs. Further observations will resolve these differences and provide a firm basis for comparison with our sample.
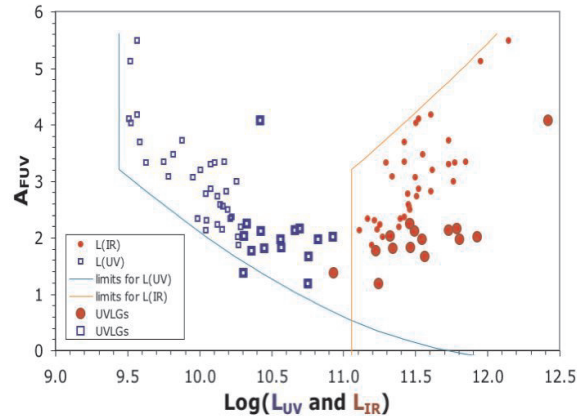

Fig. 4. Blue and red symbols are the same objects but luminosities are L_{UV} for the former and L_{IR} for the latter. The dust attenuation strongly decreases while L_{UV} increases. Part of this apparent correlation might be due to the fact that observational limits prevent us from detecting low-luminosity LBGs with low dust attenuation. The clear cut on the upper parts of the box cloud cannot be due to observational biases. We do not seem to observe UVLGs with high dust attenuations. On the other hand, the more dispersed but well-known increase of the dust attenuation with L_{IR} is observed here. Larger symbols correspond to UVLGs (Log $L_{UV} > 10.3 L_{\odot}$). Most of them have low dust attenuations but one is a ULIRG and has $A_{FUV} \sim 4$.

With the 24 μm *SPITZER* flux for the individually detected $z \sim 1$ objects, we can go a step further and check how UV dust attenuation estimations carried out from the β method compare with the better IR/UV-based estimates. This comparison has already been performed for nearby galaxies (Buat et al. 2005; Burgarella et al. 2005; Seibert et al. 2005 and references therein). Given the wide use of the β method on high redshift LBGs, it is useful to compare with our lower-redshift sample.

Using the equations in Adelberger & Steidel (2000) (deduced from Meurer et al. 1999), we estimate the IR luminosity that is used to compute A_{FUV} and the total luminosity for each LBG. We observe a small overestimation of the dust attenuation as compared to the ones estimated from *SPITZER/MIPS* data and the dust-to-UV flux ratio. The β-based mean dust attenuation estimated for our $z \sim 1$ LBG sample is $A_{FUV} = 2.76 \pm 0.13$ ($\sigma = 1.02$) while the dust-to-UV dust attenuation gives $A_{FUV} = 2.16 \pm 0.11$ ($\sigma = 0.84$) with L_{IR} from Takeuchi et al. (2005) and $A_{FUV} = 2.53 \pm 0.12$ ($\sigma = 0.94$) with L_{IR} from Chary & Elbaz (2001). The average value of the two dust-to-UV estimates is consistent with Takeuchi et al. (2005). The net effect is that total luminosities based on the β method are slightly larger than the actual values and the deduced SFRs are therefore overestimated (see next section). The mean of the ratios of the β vs. FIR/UV $A_{FUV} = 1.31 \pm 0.07$ ($\sigma = 0.52$) for Takeuchi et al. (2005) and $A_{FUV} = 1.09 \pm 0.05$ ($\sigma = 0.40$) for Chary & Elbaz's calibration.

Applying the Kaplan-Meier estimator (and using Chary & Elbaz's calibrations), we can take upper limits into account to estimate mean dust attenuations. We find moderate values $\langle A_{FUV} \rangle = 1.36 \pm 0.07$ for $M_{FUV} \leq -22$ (5 data points of which 1 is an upper limit) and $\langle A_{FUV} \rangle = 1.08 \pm 0.11$ for $M_{FUV} \leq -21$ i.e. $L_{\star}$ at $z = 3$ (35 data points of which 65% are
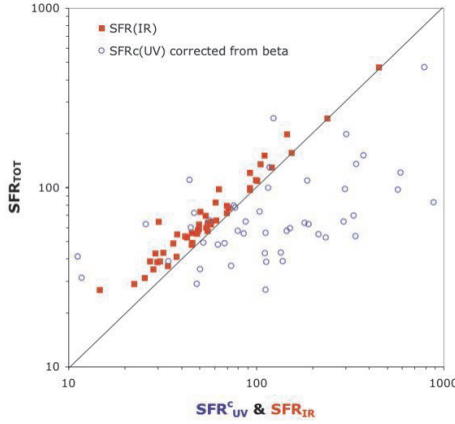
Fig. 5. Blue open circles compare SFR$^c_{UV}$ to SFR$_{TOT}$ while red filled boxes compare SFR$_{FIR}$ to SFR$_{TOT}$. Both SFRs are computed from Kennicutt (1998). The median SFR$_{FIR}$ is underestimated by about 80% and the underestimation increases at lower SFRs, which is consistent with the fact that the UV contribution (not accounted for from L_{IR}) is usually higher at low SFRs than at high SFRs. For this sample of LBG detected at 24 μm, the median value of SFR$^c_{UV}$ is over-estimated by a factor of 2–3 in average with a possible trend for the difference to increase at high SFRs. The dispersion of β-based UV SFR^{c}s (σ_{SFR} ~ 200 $M_\odot$ yr^{-1}) is much larger than IR-based SFR (σ_{SFR} ~ 30–40 $M_\odot$ yr^{-1} depending on the calibration into L_{IR}).

upper limits). Using only detections, we reached, respectively, $\langle A_{FUV}\rangle = 1.54 \pm 0.09$ and $\langle A_{FUV}\rangle = 1.59 \pm 0.18$. Since we only use a small number of bright LBGs, this is hardly comparable to the numbers quoted in the previous paragraph. However, it suggests that lower L_{FUV} LBGs have higher dust attenuations (see Fig. 4).

3.4. Star formation rates and implications for the cosmic star formation density

We estimate SFRs for our LBG sample from the IR luminosities and after applying dust corrections estimated from β and we compare them, in Fig. 5, to the total SFR: SFR$_{TOT}$ = SFR$_{UV}$ + SFR$_{IR}$ where SFR$_{UV}$ is not corrected for dust attenuation. SFR$_{TOT}$ is assumed to be the best SFR estimate and we use it as a reference. The first conclusion is that the dispersion is much larger for UV SFR^{c}s computed with β dust corrections than for IR SFRs. But the median values are also different: SFR$^c_{UV}$ = 112.3 $\pm$ 33.8 (σ = 260.9) $M_\odot$ yr^{-1} while SFR$_{IR}$ = 49.9 $\pm$ 13.1 (σ = 100.9) $M_\odot$ yr^{-1} if we use Chary & Elbaz (2001) and SFR$_{IR}$ = 30.5 $\pm$ 6.0 (σ = 46.6) $M_\odot$ yr^{-1} if we use Takeuchi et al. (2005). Median SFR$_{TOT}$ for the two above calibrations are, respectively, SFR$_{TOT}$ = 62.8 $\pm$ 13.2 (σ = 102.1) $M_\odot$ yr^{-1} and SFR$_{TOT}$ = 41.1 $\pm$ 6.3 (σ = 48.6) $M_\odot$ yr^{-1}. As expected, for LBGs detected in IR, SFR$_{IR}$ is therefore a better estimate. About 22% of our LBGs with an IR detection have SFR$_{TOT}$ > 100 $M_\odot$ yr^{-1} (using Chary & Elbaz's calibration) as compared to less than 1% in Flores et al.'s (1999) galaxy sample which confirms that our LBGs are forming stars very actively. However, none of the LBGs undetected at 24 μm is above SFR$_{TOT}$ > 100 $M_\odot$ yr^{-1}.

The higher SFRs reached when dust attenuations are computed with the UV slope β (depending on the L_{IR} calibration, +79 to +173%) lead to an overestimated contribution of LBGs to the Cosmic Star Formation Density if the same quantitative difference exists at higher redshift. However, Takeuchi et al. (2005) showed that the current assumption of a constant dust attenuation does not seem to be verified. The increase of the mean A_{FUV} from 1.3 to 2.3 from $z = 0$ to $z = 1$ means that, for a given observed FUV luminosity density, the dust-corrected star formation density would vary. Note that those mean dust attenuations cannot be compared with the numbers given for the Kaplan-Meier estimates which are biased toward large M_{FUV} LBGs while fainter LBGs seem to have larger dust attenuations in our sample. Although FIR data are not always available, it is very important that one is aware of these uncertainties when using Star Formation Densities derived from UV values corrected from the β method for LBGs with high dust attenuations, especially at high redshift where we have a very poor knowledge of actual attenuations. These ambiguities may be reduced by further study of Spitzer data, and with Herschel.

3.5. Extension to galaxies faint at 24 μm

So far, most of our arguments have been based on the 49 galaxies individually detected at 24 μm well above the completeness limit. To put the behavior of these galaxies in a broader context, we have determined average infrared flux densities for groups of galaxies by stacking. Images at 24 μm are shifted to a common center on the basis of the 24 μm coordinates if the object was well enough detected in that band, or the coordinates of the optical identification otherwise. We use sigma-clipping to eliminate surrounding sources; the level at which clipping occurs is adjusted empirically to provide the smoothest possible sky image. The quoted results are for a level of 5-σ for sources detected at 24 μm and 4-σ for undetected ones (see below), but they are not sensitive to modest adjustments in this level. In general, the resulting backgrounds have only weak structure and, where the sources are fairly bright in the infrared, the 24 μm stacked image is similar to the point spread function of the instrument. We confirmed that stacking sources of known flux density gave consistent results. These behaviors validate the procedure.

For this study, we used a total of 336 sources, selected similarly to those discussed above (but without screening for COMBO-17 type classification). We divided the sample into two groups. The first, hereafter the undetected group, includes 201 UV objects (60% of the total) for which visual inspection indicated no reliable 24 μm detection. The second (40%), hereafter the detected group, is the objects with evidence for an infrared detection; it was in turn divided into three equal subgroups according to NUV luminosity. As shown in Table 1, the two groups have very similar average NUV flux density, 1.89 μJy for the undetected and 1.63 μJy for the detected group. The average NUV luminosities are also similar, 1.3×10^{44} erg/s and 1.1×10^{44} erg/s, respectively. However, the average infrared flux densities differ by a factor of ten: 13 μJy

Table 1. Stacking analysis results.

	number	L_{UV}	$F(24\,\mu m)$	$F(B)$	$F(NUV)$	$F(B)/F(NUV)$	$F(24)/F(B)$
		10^{44} erg/s	mJy	mJy	mJy		
All detected	135	1.11	0.14	0.0018	0.0016	1.11	80
low UV	45	0.67	0.16	0.0014	0.0012	1.21	113
middle UV	45	0.99	0.16	0.0017	0.0014	1.19	95
high UV	45	1.67	0.14	0.0023	0.0024	0.98	59
Undetected	201	1.33	0.013	0.0015	0.0019	0.79	8.7

for the undetected group and 143 μJy for the detected one. There is no significant difference in average infrared flux density among the subgroups in the detected group.

These results indicate that the LBGs divide into two classes. About 40% of them are infrared bright. The average NUV flux density for this group is 1.63 μJy, so as measured in νF_ν, the NUV and 24 μm luminosities are similar. Since there is a substantial correction to total far infrared luminosity, the infrared component to the output from young stars is significant, probably accounting for the majority of the luminosity for these objects. The remaining 60% are infrared faint: νF_ν is about ten times greater in the NUV than at 24 μm, indicating that their outputs are dominated by the UV. The results of this paper apply to galaxies like those in the detected group only.

To explore other possible differences between these classes, we computed the average B (i.e. rest-frame NUV) flux densities for the same two groups and three subgroups. Although it is influenced by other factors, we take the ratio of B to NUV flux densities (or equivalently the NUV – B color) to be an indicator of the level of reddening, and the ratio of 24 μm to B flux density to measure the relative portion of the luminosity from young stars emerging in the infrared compared with the UV. The results are in Table 1. First, they demonstrate that all the galaxies in our selection fall in, or close, to the color–color LBG zone as adjusted from high z to $z \sim 1$ (see Giavalisco 2002). There is a trend for LBGs with a high 24/B ratio to present a high B/NUV, which is consistent with the relation for the UV slope β and the FIR/UV ratio found by Meurer et al. (2000) on a sample of local starburst galaxies. An analysis based on detections is required to check whether Meurer et al.'s law can be applied safely to those LBGs while we showed in the previous section that it provides dispersed SFRs for the detected sample. Finally, the amount of dust attenuation for the undetected group is very low ($A_{FUV} \sim 0.5$–0.6 for a mean Log $L_{TOT} \approx 10.5$) which corresponds to LBGs with the lowest reddening found by Adelberger & Steidel (2000). This very low reddening is consistent with the very blue UV slope $\beta \approx -2.4$. If confirmed, this would mean that about half of the LBGs do not contain large amounts of dust.

4. Conclusions

We use multi-wavelength data in the CDFS to define the first large sample of Lyman Break Galaxies at $z \sim 1$; *GALEX* is used to observe the Lyman break. Redshifts are taken from spectra and from COMBO 17. Quantitative morphologies

(Lauger et al. 2005a) are estimated from high spatial resolution images. Finally, dust attenuations and total luminosities are computed from *SPITZER* measurements at 24 μm extrapolated to get the total IR luminosity.

The main results of this analysis are:

1. We detect ∼300 LBGs in the range $9.3 \leq \text{Log } L_{FUV}[L_\odot] \leq 11.0$, i.e. well into the UVLG class as defined by Heckman et al. (2005). For the same objects, Log $L_{IR} \geq 11\ L_\odot$, which means that almost all the LBGs with a *SPITZER* confirmed detection are LIRGs (and 1 ULIRG) at $z \sim 1$.

2. LBGs at $z \sim 1$ are mainly disk-dominated galaxies (75%) with a small contribution of interacting/merging galaxies (22%) and a negligible (3%) fraction are spheroids. The morphologies of our LBG sample are consistent with star-forming galaxies.

3. The FUV dust attenuation appears to be anti-correlated with the observed FUV luminosity. Part of this correlation might be due to observational limits at 24 μm. However, non-detection of LBG with high L_{FUV} and high A_{FUV} cannot be explained by observational biases.

4. About 40% of our sample of LBGs is detected at 24 μm. These objects also show evidence for reddening in their UV continua. The remaining 60% of the sample are on average an order of magnitude less luminous in the infrared compared with the rest frame near UV. Their UV continua also appear to be significantly less reddened.

5. Dust corrections of our IR-bright LBG sample computed via the β method are over-estimated by ∼0.2 mag. if we use Chary & Elbaz (2001) to compute L_{IR} and by ∼0.6 mag. if we use Takeuchi et al. (2005).

6. Dust attenuations estimated by the β method for such galaxies lead to overestimation of the SFRs at $z \sim 1$ by a factor of 2 to 3, depending on the calibration of the 24 μm flux to L_{IR} while IR-based SFRs are of the same order as SFR$_{TOT}$.

7. By using the stacking method, we find that LBGs non detected at 24 μm seem to have very low dust attenuations.

References

Adelberger, K. L., & Steidel, C. C. 2000, ApJ, 544, 218

Baker, A. J., Lutz, D., Genzel, R., Tacconi, L. J., & Lehnert, M. D. 2001, A&A, 372, 37

Bell, E. F. 2002, ApJ, 577, 150

Bell, E. F., Papovich, C., Wolf, C., et al. 2005, ApJ, 625, 23

Blain, A. W., Smail, I., Ivison, R. J., & Kneib, J.-P. 1999, MNRAS, 302, 632

Buat, V., Iglesias-Pramo, J., Seibert, M., et al. 2005, ApJ, 619, L51

Burgarella, D., Buat, V., Donas, J., Milliard, B., & Chapelon, S. 2001, AJ, 369, 421

Burgarella, D., Buat, V., Small, T., et al. 2005, MNRAS, 360, 1413

Calzetti, D., Kinney, A. L., & Storchi-Bergmann, T. 1994, ApJ, 429, 582

Chapman, S. C., Scott, D., Steidel, C. C., et al. 2000, MNRAS, 319, 318

Chary, R., & Elbaz, D. 2001, ApJ, 556, 562

Conselice, C. J., Blackburne, J. A., & Papovich, C. 2005, ApJ, 620, 564

Dale, D. A., et al. 2005, ApJ, in press [`arXiv:astro-ph/0507645`]

Dale, D. A., & Helou, G. 2002, ApJ, 576, 159

Elbaz, D., & Cesarsky, C. J. 2003, Science, 300, 270

Flores, H., Hammer, F., Thuan, T. X., et al. 1999, ApJ, 517, 148

Giavalisco, M., Steidel, C. C., & Macchetto, F. D. 1996, ApJ, 470, 189

Giavalisco, M. 2002, ARA&A, 40, 579

Goldader, J. D., Meurer, G., Heckman, T. M., et al. 2002, ApJ, 568, 651

Heckman, T. M., Hoopes, C. G., Seibert, M., et al. 2005, ApJ, 619, L35

Huang, J.-S., et al. 2005, ApJ, in press [`arXiv:astro-ph/0507685`]

Ivison, R. J., Smail, I., Bentz, M., et al. 2005, MNRAS, 362, 535

Kennicutt, R. C. 1988, ARA&A, 36, 189

Labbé, I., Huang, J., Franx, M., et al. 2005, ApJ, 624, L81

Lauger, S., Burgarella, D., & Buat, V. 2005a, A&A, 434, 77

Lauger, S., et al. 2005b, A&A, submitted

Le Fèvre, O., Vettolani, G., Paltani, S., et al. 2004, A&A, 428, 1043

Lowenthal, J. D., Koo David, C., Guzman, R., et al. 1997, ApJ, 481, 673

Madau, P., Ferguson, H. C., Dickinson, M. E., et al. 1996, MNRAS, 283, 1388

Martin, D. C., Fanson, J., Schiminovich, D., et al. 2005, ApJ, 619, L1

Meurer, G. R., Heckman, T. M., & Calzetti, D. 1999, ApJ, 521, 64

Moorwood, A. F. M., van der Werf, P. P., Cuby, J. G., & Oliva, E. 2000, A&A, 362, 9

Pérez-González, P. G., et al. 2005, ApJ, in press [`arXiv:astro-ph/0505101`]

Pettini, M., Steidel, C. C., Adelberger, K. L., Dickinson, M., & Giavalisco, M. 2000, ApJ, 528, 96

Pettini, M., Shapley, A. E., Steidel, C. C., et al. 2001, ApJ, 554, 981

Rieke, G. H., Young, E. T., Engelbracht, C. W., et al. 2004, ApJS, 154, 25

Seibert, M., Martin, D. C., Heckman, T. M., et al. 2005, ApJ, 619, L59

Steidel, C. C., & Hamilton, D. 1993, AJ, 105, 201

Steidel, C. C., Giavalisco, M., Pettini, M., Dickinson, M., & Adelberger, K. L. 1996, ApJ, 462, L17

Teplitz, H., McLean, I. S., Becklin, E. E., et al. 2000, ApJ, 533, 65

Takeuchi, T. T., Buat, V., Iglesias-Paramo, J., Boselli, A., & Burgarella, D. 2005, A&A, 432, 423

Takeuchi, T. T., Buat, V., & Burgarella, D. 2005, A&A, 440, L17

Vanzella, E., Cristiani, S., Dickinson, M., et al. 2005, A&A, 434, 53

Wolf, C., Meisenheimer, K., Kleinheinrich, M., et al. 2004, A&A, 421, 913

Wolf, C., Bell, E. F., McIntosh, D. H., et al. 2005, ApJ, 630, 771

Zheng, X. Z., Hammer, F., Flores, H., Assmat, F., & Pelat, D. 2004, A&A, 421, 847